

# Multiple Control Mechanisms for Pyrimidine-Mediated Regulation of *pyrBI* Operon Expression in *Escherichia coli* K-12

CHONGGUANG LIU AND CHARLES L. TURNBOUGH, JR.\*

Department of Microbiology, University of Alabama at Birmingham, Birmingham, Alabama 35294

Received 3 October 1988/Accepted 20 March 1989

Expression of the *pyrBI* operon of *Escherichia coli* K-12, which encodes the subunits of the pyrimidine biosynthetic enzyme aspartate transcarbamylase, is negatively regulated over a several-hundredfold range by pyrimidine availability. This regulation occurs, at least in large part, through a UTP-sensitive attenuation control mechanism in which transcriptional termination at the *pyrBI* attenuator, a  $\rho$ -independent transcriptional terminator located immediately upstream of the *pyrB* structural gene, is regulated by the relative rates of transcription and translation within the *pyrBI* leader region. There is suggestive evidence that an additional, attenuator-independent control mechanism also contributes to this regulation. To measure the level of regulation that occurs through the attenuation and attenuator-independent control mechanisms, we constructed a mutant strain in which a 9-base-pair deletion was introduced into the attenuator of the chromosomal *pyrBI* operon. This deletion, which removes the run of thymidine residues at the end of the attenuator, completely abolishes  $\rho$ -independent transcriptional termination activity. When the mutant strain was grown under conditions of pyrimidine excess, the level of operon expression was 51-fold greater than that of an isogenic *pyrBI*<sup>+</sup> strain. Under conditions of pyrimidine limitation, operon expression was increased an additional 6.5-fold in the mutant. These results demonstrate that the attenuation control mechanism is primarily responsible for pyrimidine-mediated regulation but that there is a significant contribution by an attenuator-independent control mechanism.

In *Escherichia coli* K-12, the de novo synthesis of UMP, the precursor of all pyrimidine nucleotides, is catalyzed by six enzymes encoded by six unlinked genes and small operons. The expression of these genes and operons is noncoordinately regulated by the intracellular levels of uridine or cytidine nucleotides (15). One of the small operons, the *pyrBI* operon, encodes the catalytic (*pyrB*) and regulatory (*pyrI*) subunits of the allosteric enzyme aspartate transcarbamylase (ATCase; EC 2.1.3.2). Expression of the *pyrBI* operon is negatively regulated over a several-hundredfold range by pyrimidine availability. Recent studies indicate that most of this regulation occurs through a UTP-sensitive attenuation control mechanism (9, 19, 23). In this mechanism, transcriptional termination at the *pyrBI* attenuator, a  $\rho$ -independent transcriptional terminator located 23 base pairs (bp) upstream of the *pyrB* gene (Fig. 1), is regulated by the relative rates of transcription and translation within the *pyrBI* leader region (6, 8, 19). According to the current model for attenuation control, low intracellular levels of UTP cause RNA polymerase to pause during the synthesis of uridine-rich regions in the leader transcript. This pausing provides time for a ribosome to initiate the translation of an open reading frame for a 44-amino-acid leader polypeptide and catch up to RNA polymerase before the transcription of the attenuator. When RNA polymerase eventually transcribes the attenuator, the adjacent translating ribosome will prevent the formation of the attenuator-encoded RNA hairpin, which is required for transcriptional termination, resulting in readthrough transcription into the *pyrBI* structural genes (18).

In several of the studies describing the attenuation control mechanism, data are presented which suggest that an additional, attenuator-independent control mechanism contrib-

utes to pyrimidine-mediated regulation of *pyrBI* operon expression. For example, the expression of gene fusions constructed by joining the *pyrBI* promoter-regulatory region preceding the attenuator to a reporter gene like *lacZ* or *galK* can be derepressed two- to fourfold by pyrimidine limitation (9, 19). In another experiment, it was shown that the insertion of a restriction fragment containing just the *pyrBI* leader region (including the attenuator) into a site between the *lac* promoter and the *lacZ* gene permits regulation of *lacZ* expression by pyrimidine availability, but only over a range approximately one-tenth of that observed with the *pyrBI* operon (6). This result suggests that attenuation control is not sufficient to account for all of the observed regulation. Although these results indicate the involvement of a second control mechanism, it is unlikely that they reflect in a quantitative way the contribution of the two control mechanisms to regulation. In all cases, the gene fusions were carried on multicopy plasmids, a situation in which the range of regulation of *pyrBI* expression is reduced severalfold (19). In addition, the different genetic environments of the fusions probably affect the level of regulation.

In this study, we have attempted to measure as precisely as possible the contributions of the attenuation and attenuator-independent control mechanisms to pyrimidine-mediated regulation. This was accomplished by introducing a 9-bp deletion mutation into the attenuator of the chromosomal *pyrBI* operon. This deletion completely abolishes  $\rho$ -independent transcriptional termination activity at the mutant attenuator but does not appear to affect the operon in any other way. The effect of the attenuator deletion on *pyrBI* expression was measured by assaying ATCase levels in mutant and wild-type cells grown under conditions of pyrimidine excess or limitation. The results clearly show the major role of the attenuation control mechanism in regulation and

\* Corresponding author.

provide convincing evidence for an additional, attenuator-independent control mechanism.

### MATERIALS AND METHODS

**Bacterial strains.** All strains used are *E. coli* K-12 and are described in Table 1. Bacteriophage P1-mediated transductions used in strain constructions were performed essentially as described previously (14).

**Plasmid constructions.** Plasmids constructed in this study are shown in Fig. 2. Plasmid pBHM42 was made by inserting a 177-bp *EcoRI* fragment containing the transcriptional terminator of the *E. coli* *rrnB* operon into the unique *EcoRI* site of plasmid pBHM9 (19). Plasmid pBHM161 was constructed by inserting a 1.3-kilobase (kb) kanamycin resistance cassette (Pharmacia, Inc.) into the *PvuII* site of the *pyrB* gene of plasmid pBHM42. The construction of plasmid pBHM141 is described in Results.

**DNA preparations, restriction digests, ligations, and transformations.** DNA preparation, restriction digestion, ligations, and transformations were performed as previously described (18, 19). Restriction endonucleases, T4 DNA ligase, T4 polynucleotide kinase, and the Klenow fragment of DNA polymerase I were obtained from New England Biolabs. The oligodeoxynucleotide used for in vitro mutagenesis was 5'-TCGAGGGGCCCCAGGCGTC.

**In vitro oligonucleotide-directed mutagenesis.** Oligonucleotide-directed mutagenesis was performed by following the gapped heteroduplex procedure of Bauer et al. (3). The single-stranded template DNA was isolated from recombinant bacteriophage M13mp9am (amber mutations in genes I and II) in which the 1-kb *RsaI* fragment of plasmid pBHM42 has been inserted into the *SmaI* site of the phage genome. The 1-kb *RsaI* fragment contains the promoter-regulatory region of the *pyrBI* operon. Replicative-form DNA was isolated from M13mp11 and digested with *HindIII* and *EcoRI*. For the annealing reaction, the template and replicative-form DNA were mixed in equimolar amounts (0.2 pmol each) in a final volume of 30  $\mu$ l of buffer A (20 mM Tris hydrochloride, pH 7.5, 10 mM MgCl<sub>2</sub>, 100 mM NaCl, 1 mM dithiothreitol). This mixture was boiled for 3 min and then slowly cooled to 65°C. After addition of 40 pmol (10  $\mu$ l) of the mutagenic 5'-phosphorylated oligonucleotide, the mixture was cooled slowly to room temperature and then placed on ice for 10 min. For the elongation reaction, 40  $\mu$ l of elongation mixture (20 mM Tris hydrochloride, pH 7.5, 10 mM MgCl<sub>2</sub>, 10 mM dithiothreitol, 1 mM rATP, 1 mM each deoxynucleoside triphosphates, 3 U of T4 DNA ligase, 2.5 U of Klenow fragment of DNA polymerase I) was added to the annealed DNA. This mixture was incubated at 16°C for 30 min and then at room temperature for an additional 3.5 h. A

portion of the mixture was used to transform strain JM105. Transformants were screened for the absence of  $\alpha$  complementation (13). DNA was isolated from putative mutant phage, and the presence of the oligonucleotide-directed mutation was confirmed by DNA sequence analysis (20). The sequence of the entire *pyrBI* promoter-regulatory region was determined to verify that additional changes were not introduced by the mutagenesis procedure.

**Southern hybridization.** Chromosomal and plasmid DNA was subjected to restriction enzyme digestion. The digested DNA was prepared for hybridization and probed as described by Maniatis et al. (11) with modifications as indicated in the text. The DNA was transferred from a 1% agarose gel to nitrocellulose filter paper by vacuum blotting. The probes used were <sup>32</sup>P-labeled DNA fragments complementary to the 758-bp *PvuII* fragment of plasmid pBHM42, which were synthesized by a random-priming procedure (7), and 5'-<sup>32</sup>P-labeled synthetic oligodeoxynucleotides, which are described in the text. The oligonucleotide probes were labeled with T4 polynucleotide kinase and [ $\gamma$ -<sup>32</sup>P]ATP (5,000 Ci/mmol, Amersham Corp.).

**In vitro transcription.** The preparation of purified RNA polymerase holoenzyme was done as previously described (23). Restriction fragments used as DNA templates were separated by 8% polyacrylamide gel electrophoresis, extracted from the gel as previously described (12), and further purified by salt elution from a DEAE-cellulose (Whatman DE52) column. Reaction mixtures (50  $\mu$ l) contained 20 mM Tris hydrochloride (pH 7.9), 10 mM MgCl<sub>2</sub>, 50 mM KCl, 0.1 mM disodium EDTA, 0.1 mM dithiothreitol, 0.2 mM GTP, 0.2 mM CTP, 0.2 mM UTP, 0.2 mM [ $\gamma$ -<sup>32</sup>P]ATP (10 Ci/mmol, ICN Pharmaceuticals Inc.), 10 nM DNA template, and 50 nM RNA polymerase. Reaction mixtures lacking ribonucleoside triphosphates were preincubated for 5 min at 37°C. Reactions were initiated by the addition of the nucleoside triphosphates, and the mixtures were incubated for 5 min at 37°C. Heparin (Sigma Chemical Co.) was then added to a final concentration of 0.1 mg per ml, and the mixtures were incubated for an additional 10 min. Reactions were terminated by the addition of 0.25 ml of ice-cold 0.3 M sodium acetate (pH 5.2), 1 mM disodium EDTA, and 40  $\mu$ g of sonicated calf thymus DNA per ml. The RNA transcripts in the reaction mixture were precipitated by adding 2.5 volumes of 95% ethanol and placing the sample in a dry ice-ethanol bath for 15 min. The RNA was collected by centrifugation, dissolved in 50  $\mu$ l of water, dried in vacuo, and dissolved in 99% formamide containing 0.1% each bromophenol blue and xylene cyanol. The transcripts were separated by electrophoresis in a 10% polyacrylamide-TBE (0.1 M Tris borate [pH 8.3]-2 mM disodium EDTA) sequenc-

TABLE 1. *E. coli* K-12 strains

Strain	Genotype	Source
AT2473	HfrH <i>thi-1 relA1 car-94</i> $\lambda^-$	B. Bachmann (CGSC 4512)
JM105	$\Delta(lac-pro)$ <i>thi rpsL sbcB15 endA hspR4</i> (F' <i>traD36 proAB lacI<sup>q</sup>Z<math>\Delta</math>M15</i> )	J. Messing
JC7623	<i>recB21 recC22 sbcB15 arg ara his leu pro thr</i>	G. Walker (25)
MC4100	F <sup>-</sup> <i>araD139 <math>\Delta(argF-lac)U169 rpsL150 thiA1 relA1 deoC1 ptsF25 ffbB5301 rbsR</math></i>	M. Casadaban (5)
CLT42	MC4100 <i>ara<sup>+</sup> car-94</i>	This laboratory (19)
CLT67	JC7623 <i>pyrB482::kan</i>	This paper
CLT68	MC4100 <i>pyrB482::kan</i>	P1 (CLT67) $\times$ MC4100
CLT69	JC7623 $\Delta$ <i>pyrBa483<sup>a</sup></i>	This paper
CLT70	MC4100 $\Delta$ <i>pyrBa483</i>	P1 (CLT69) $\times$ CLT68
CLT71	CLT70 <i>ara<sup>+</sup> car-94</i>	P1 (AT2473) $\times$ CLT70

<sup>a</sup> *pyrBa* is used to designate the attenuator preceding the *pyrB* structural gene as recommended by Bachmann and Low (2).

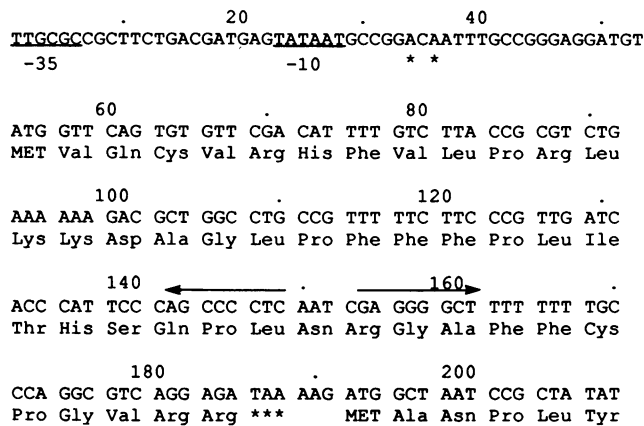


FIG. 1. Nucleotide sequence and encoded polypeptides of the *pyrBI* promoter-regulatory region. Only the antisense strand is shown; numbering is from the 5' end. The -10 and -35 regions of the *pyrBI* promoter, previously designated promoter P<sub>2</sub> (23), are underlined and labeled. Approximately 99% of *pyrBI* transcripts are initiated at this promoter in vivo; the asterisks below bp 34 and 36 indicate the two sites at which initiation occurs under the in vitro transcription conditions used in this study (J. P. Donahue and C. L. Turnbough, Jr., unpublished data). The leader polypeptide is encoded by bp 54 through 185, and the *pyrB* structure gene begins at bp 192. The hyphenated dyad symmetry of the *pyrBI* attenuator (bp 142 through 168) is indicated by horizontal arrows. The  $\Delta$ *pyrBa483* mutation deletes bp 161 through 169.

ing gel containing 7 M urea and were visualized by autoradiography.

**Media and culture methods.** Cells used for ATCase assays were grown in N<sup>-</sup>C<sup>-</sup> medium (1) supplemented with 10 mM NH<sub>4</sub>Cl, 0.4% glucose, 0.015 mM thiamine hydrochloride, 1 mM arginine, and either 1 mM uracil or 0.25 mM UMP. Cultures (25 ml in a 125-ml flask) were grown at 30°C with shaking. The solid media used in strain constructions were LB medium (14), with ampicillin (25 µg/ml) or kanamycin sulfate (50 µg/ml) added when required, and N<sup>-</sup>C<sup>-</sup> medium containing 10 mM NH<sub>4</sub>Cl, 0.015 mM thiamine hydrochloride, and 1.5% Difco agar, with 0.4% glucose, 1% L-arabinose, 0.2 mM uracil, and amino acids at 0.3 mM each added as required. Growth on solid media was at 37°C.

**ATCase assay.** ATCase activity in cells harvested from exponential-phase cultures ( $A_{650} = 0.5$  as measured with a Gilford model 260 spectrophotometer) was assayed as previously described (18).

## RESULTS

**Construction of the  $\Delta$ *pyrBa483* mutation.** All  $\rho$ -independent transcriptional terminators consist of a G+C-rich region of hyphenated dyad symmetry followed immediately by a long run of thymidine residues (corresponding to uridine residues in the transcript) (16). Deletion of the entire run of thymidine residues has been shown to abolish all termination activity in vivo and in vitro (10). To inactivate the *pyrBI* attenuator, we constructed a mutation, designated  $\Delta$ *pyrBa483*, which deletes all eight thymidine residues at the end of this  $\rho$ -independent terminator. The deletion also includes one additional residue downstream of the run of thymidines, which was removed to maintain the same reading frame for the *pyrBI* leader polypeptide (Fig. 1). The mutation was made in a recombinant M13 phage by oligonucleotide-directed mutagenesis as described in Materials and Methods.

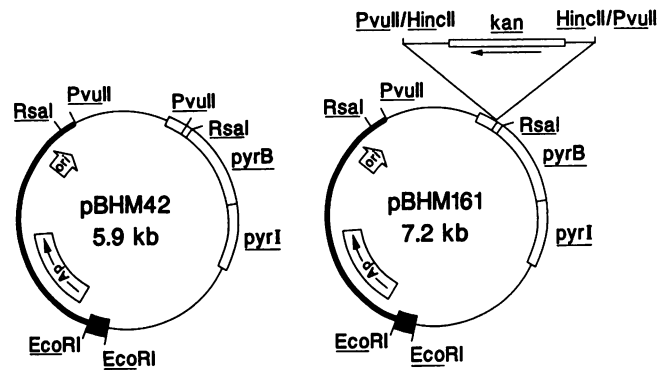


FIG. 2. Plasmids used in strain constructions. Plasmid pBHM42 contains a 3.4-kb segment of the *E. coli* chromosome carrying the *pyrBI* operon, the 2.3-kb *PvuII*-*EcoRI* fragment of plasmid pBR322 (thick line), and a 177-bp *EcoRI* restriction fragment containing the transcriptional terminator of the *E. coli* *rrnB* operon (closed box). Plasmid pBHM141 (not shown) is identical to plasmid pBHM42 except for a 9-bp deletion ( $\Delta$ *pyrBa483*) in the attenuator preceding the *pyrBI* structural genes. Plasmid pBHM161 is a derivative of plasmid pBHM42 in which a kanamycin resistance cassette has been inserted into the *PvuII* site of the *pyrB* gene. Only relevant restriction sites are shown in the diagrams. Arrows indicate direction of transcription.

The  $\Delta$ *pyrBa483* mutation was then excised from replicative-form phage DNA as part of a 749-bp *PvuII* fragment that includes the *pyrBI* promoter-regulatory region. This fragment was used to replace the equivalent 758-bp *PvuII* fragment of the *pyrBI*-containing plasmid pBHM42 (Fig. 2) to generate plasmid pBHM141.

**Introduction of the  $\Delta$ *pyrBa483* mutation into the chromosomal *pyrBI* operon.** The introduction of the  $\Delta$ *pyrBa483* mutation into the *pyrBI* operon of the chromosome of strain MC4100, the parent strain used in our laboratory, was done in several steps. First, we constructed a strain carrying a selectable *pyrB* mutation by transformation of strain JC7623 with *EcoRI*-digested plasmid pBHM161 (*pyrB482::kan*) (Fig. 2). Strain JC7623 (*recB21 recC22 sbcB15*) was used as the recipient because it can be readily transformed with linearized DNA (25). A kanamycin-resistant pyrimidine-auxotrophic transformant was isolated and designated strain CLT67. The *pyrB482::kan* mutation of this strain was then transferred to strain MC4100 by P1-mediated transduction to generate strain CLT68.

The next step was to replace the *pyrBI* operon of strain CLT68 (MC4100 *pyrB482::kan*) with the operon carried by plasmid pBHM141 ( $\Delta$ *pyrBa483*). This replacement was done by first transforming strain CLT67 (JC7623 *pyrB482::kan*) with *EcoRI*-digested plasmid pBHM141. A pyrimidine-prototrophic kanamycin-sensitive transformant was isolated and designated strain CLT69 (JC7623  $\Delta$ *pyrBa483*). The  $\Delta$ *pyrBa483* mutation of this strain was moved into strain CLT68 (MC4100 *pyrB482::kan*) by P1-mediated transduction. A pyrimidine-prototrophic kanamycin-sensitive transductant was designated CLT70 (MC4100  $\Delta$ *pyrBa483*). A pyrimidine-auxotrophic derivative of strain CLT70 was constructed by introducing the *car-94* mutation from strain AT2473 by P1-mediated transduction. This derivative was designated strain CLT71 (MC4100  $\Delta$ *pyrBa483 ara*<sup>+</sup> *car-94*).

**Confirmation of the chromosomal  $\Delta$ *pyrBa483* mutation.** The presence of the  $\Delta$ *pyrBa483* mutation in the *pyrBI* operon of strain CLT70 was demonstrated by Southern hybridization. Chromosomal DNA was prepared from strains MC4100

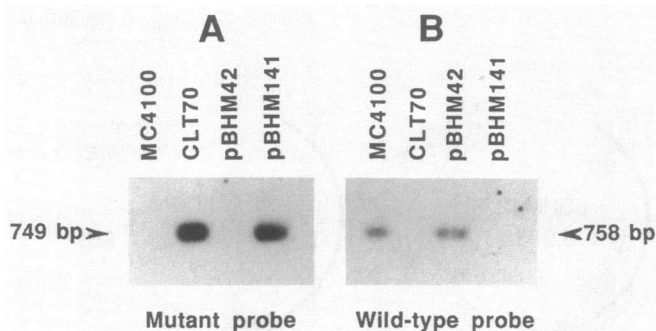


FIG. 3. Autoradiograms of Southern blots used to detect the *pyrBI* attenuator deletion  $\Delta$ *pyrBa483*. Chromosomal DNA from strains MC4100 (*pyrBa*<sup>+</sup>) and CLT70 ( $\Delta$ *pyrBa483*) and plasmids pBHM42 (*pyrBa*<sup>+</sup>) and pBHM141 ( $\Delta$ *pyrBa483*) were digested to completion with *Pvu*II. Two identical blots were prepared in which 50  $\mu$ g of chromosomal DNA or 30 ng of plasmid DNA was loaded in the indicated lanes of the agarose gel. The blotted DNA was probed with either the 5'-<sup>32</sup>P-labeled mutagenic oligonucleotide (A) or a 5'-<sup>32</sup>P-labeled oligonucleotide with the same sequence as nucleotides 156 through 174 in Fig. 1 (B). Hybridizations were done for 16 h at either 50 (A) or 42°C (B). The high-temperature washes were done twice for 30 min each at either 50 (A) or 40°C (B). Only the region of each autoradiogram containing bands is shown.

(*pyrBa*<sup>+</sup>) and CLT70 ( $\Delta$ *pyrBa483*), digested with *Pvu*II, and probed with radiolabeled oligonucleotides which will hybridize to either the mutant or wild-type *pyrBI* attenuator region. As a control, plasmids pBHM42 (*pyrBa*<sup>+</sup>) and pBHM141 ( $\Delta$ *pyrBa483*) were digested with *Pvu*II and included in the Southern blots. The data show that the oligonucleotide with the mutant attenuator sequence hybridized specifically with the 749-bp *Pvu*II fragments from strain CLT70 and plasmid pBHM141, while the oligonucleotide with the wild-type attenuator sequence hybridized only with the 758-bp *Pvu*II fragments from strain MC4100 and plasmid pBHM42 (Fig. 3). These data confirm the presence of the  $\Delta$ *pyrBa483* mutation in the chromosome of strain CLT70.

To show that the introduction of the  $\Delta$ *pyrBa483* mutation into the chromosome of strain CLT70 was not accompanied by large insertions, deletions, or rearrangements, we compared the *pyrBI* regions of this strain and the wild-type strain MC4100 by Southern hybridization. Chromosomal DNA from the two strains was digested with either *Pst*I, *Pst*I and *Bgl*III, or *Pvu*II and hybridized with a probe complementary to the 758-bp *Pvu*II fragment of the *pyrBI* promoter-regulatory region. The restriction sites of these enzymes in the *pyrBI* region are shown at the bottom of Fig. 4. These enzymes were chosen because they would allow detection of large changes in the *pyrBI* region of strain CLT70. The data show that there are no large differences in the sizes of the fragments from the two strains, indicating that the introduction of the  $\Delta$ *pyrBa483* mutation occurred by homologous recombination.

**Effect of the  $\Delta$ *pyrBa483* mutation on in vitro transcription of the *pyrBI* promoter-regulatory region.** To confirm that the  $\Delta$ *pyrBa483* mutation abolishes transcriptional termination at the *pyrBI* attenuator, we transcribed the wild-type and mutant *pyrBI* promoter-regulatory regions in vitro (Fig. 5). The data show that the wild-type attenuator terminated essentially all *pyrBI* transcripts, as was previously shown (23). Termination apparently occurs at the last two thymidine residues at the end of the attenuator (J. P. Donahue and C. L. Turnbough, Jr., unpublished data). On the other hand,

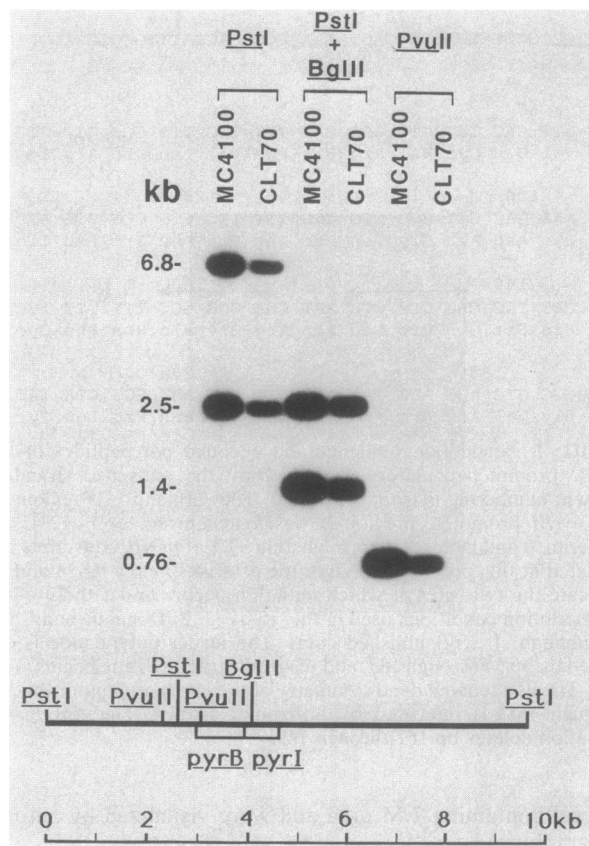


FIG. 4. Autoradiogram of a Southern blot used to compare the *pyrBI* regions of strains MC4100 (*pyrBa*<sup>+</sup>) and CLT70 ( $\Delta$ *pyrBa483*). Chromosomal DNA was digested with either *Pst*I, *Pst*I and *Bgl*III, or *Pvu*II and loaded in the indicated lanes of the agarose gel (approximately 30  $\mu$ g from strain MC4100 and 15  $\mu$ g from strain CLT70). The blotted DNA was probed with <sup>32</sup>P-labeled DNA fragments complementary to the 758-bp *Pvu*II fragment of the *pyrBI* promoter-regulatory region. Hybridizations and washes were done as described previously (11). The sizes of the restriction fragments were determined by comparison with unlabeled DNA standards which were run in the same gel. A restriction map of the *pyrBI* region is shown at the bottom of the figure.

the  $\Delta$ *pyrBa483* mutation appeared to eliminate all termination activity as indicated by the absence of any attenuated transcripts, which presumably would be between 125 and 135 nucleotides long. Nearly all of the *pyrBI* transcripts are extended to the end of the mutant template.

**Effect of the  $\Delta$ *pyrBa483* mutation on the expression and regulation of the *pyrBI* operon.** The effect of the  $\Delta$ *pyrBa483* mutation on *pyrBI* expression was determined by measuring the ATCase levels in strains CLT42 (*pyrBa*<sup>+</sup> *car-94*) and CLT71 ( $\Delta$ *pyrBa483* *car-94*). Both strains are pyrimidine auxotrophs because the *car-94* mutation inactivates the first enzyme of the pyrimidine biosynthetic pathway. The strains were grown in a glucose-minimal salts medium containing either uracil or UMP as the pyrimidine source. Growth on uracil causes repressed *pyr* gene expression, whereas growth on UMP, which is only slowly utilized by the cells, results in pyrimidine limitation and derepressed *pyr* gene expression.

The results show that in uracil-grown cells the level of ATCase activity in strain CLT71 was 51-fold greater than that in strain CLT42, while in UMP-grown cells the enzyme levels were similar (just 5% higher in strain CLT71) (Table

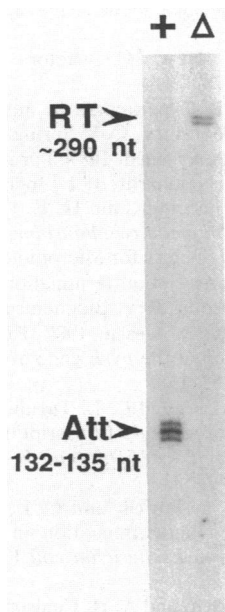


FIG. 5. The effect of the  $\Delta pyrBa483$  mutation on in vitro transcription of the *pyrBI* promoter-regulatory region. An autoradiogram of a 10% polyacrylamide sequencing gel used to separate  $5'$ - $^{32}P$ -labeled *pyrBI* transcripts synthesized in vitro is shown. The DNA templates used were either the 758-bp *PvuII* fragment of plasmid pBHM42 (*pyrBa*<sup>+</sup>) (+ lane) or the 749-bp *PvuII* fragment of plasmid pBHM141 ( $\Delta pyrBa483$ ) ( $\Delta$  lane). The sizes of the attenuated (Att) and readthrough (RT) transcripts were determined by coelectrophoresis with RNA standards (data not shown). Note that the 133- and 134-nucleotide (nt) attenuated transcripts, which are initiated at different sites (Fig. 1), comigrated in this gel (V. W. Pollard and C. L. Turnbough, Jr., unpublished data).

2). The similar enzyme levels in the strains grown on UMP indicate that the  $\Delta pyrBa483$  mutation did not significantly affect the efficiency of translation or the stability of the full-length *pyrBI* transcript; the small, but reproducible, difference in enzyme levels may indicate that even under pyrimidine-limiting growth conditions approximately 5% of the *pyrBI* transcripts are terminated at the attenuator of strain CLT42. The 51-fold difference in ATCase activity in the two strains grown on uracil was due to the different levels of readthrough transcription into the *pyrBI* structural genes that occurred in the presence or absence of a functional *pyrBI* attenuator. Therefore, this difference measures the contribution of attenuation control to pyrimidine-mediated regulation of operon expression.

Although the  $\Delta pyrBa483$  mutation in strain CLT71 eliminated attenuator-dependent regulation, expression of the

TABLE 2. Effect of the  $\Delta pyrBa483$  mutation on ATCase synthesis<sup>a</sup>

Strain (genotype)	ATCase activity (nmol/min per mg)		
	Repressed <sup>b</sup>	Derepressed <sup>c</sup>	Fold derepression
CLT42 ( <i>car-94 pyrBa</i> <sup>+</sup> )	18.2	5,670	312
CLT71 ( <i>car-94 ΔpyrBa483</i> )	920	5,970	6.5

<sup>a</sup> Doubling times were 64 min for strain CLT42 and 70 min for strain CLT71 when grown on uracil; doubling times were 114 min for both strains when grown on UMP.

<sup>b</sup> Cells grown on uracil; mean of two experiments.

<sup>c</sup> Cells grown on UMP; mean of two experiments.

*pyrBI* operon in this strain was still significantly affected by pyrimidine availability. The level of ATCase activity in cells grown on UMP was 6.5-fold greater than that in cells grown on uracil. This result provides strong evidence for a second pyrimidine-sensitive control mechanism for the regulation of *pyrBI* expression.

## DISCUSSION

The results presented in this paper demonstrate that there are multiple control mechanisms involved in the pyrimidine-mediated regulation of *pyrBI* operon expression. The previously described UTP-sensitive attenuation control mechanism accounts for most of the regulation: approximately 50-fold of the greater than 300-fold regulation observed in cells grown under the conditions of pyrimidine limitation or excess used in this study. An attenuator-independent control mechanism(s) appears to be responsible for the remainder of the regulation: approximately 6.5-fold.

The nature of this second control mechanism is not known. The fact that gene fusions between the beginning of the *pyrBI* leader region and a reporter gene can be regulated over a severalfold range by pyrimidine availability indicates that the site of regulation is upstream of the attenuator, perhaps at the *pyrBI* promoter. We previously reported that decreasing the concentration of UTP from 200 to 20  $\mu M$  stimulated transcription from this promoter severalfold in vitro (23). Perhaps this second control mechanism involves such a stimulation in vivo. We also previously showed that guanosine tetraphosphate, at least at high intracellular levels, is a negative regulatory effector of *pyrBI* expression (22). Because pyrimidine limitation apparently causes a decrease in the basal level of guanosine tetraphosphate in cells grown under conditions similar to those used in this study (17), it is possible that such an effect could account for or contribute to the observed attenuator-independent control. To test this as well as other possible control mechanisms, it will be necessary to isolate and characterize mutations that affect attenuator-independent control.

The discovery of the multiple control mechanisms for the *pyrBI* operon permits an interesting comparison with the pyrimidine-mediated control mechanisms of the *pyrE* and *pyrF* genes of *E. coli*. The expression of these genes, which encode the enzymes that catalyze the last two steps in UMP biosynthesis, is also regulated by a uridine nucleotide effector. In the case of the *pyrE* gene, this regulation occurs over an approximately 30-fold range almost exclusively through a UTP-sensitive attenuation control mechanism that is essentially the same as that described for the *pyrBI* operon (4, 17). Less than twofold of the pyrimidine-mediated regulation of *pyrE* expression appears to occur through an attenuator-independent mechanism (17). In contrast, regulation of *pyrF* expression occurs over only an approximately sixfold range by a mechanism that does not involve attenuation control (24). Although the exact identity of the uridine nucleotide effector of *pyrF* expression is unknown, UTP appears to be the most likely candidate (21). The similarities between the *pyrBI* and *pyrE* attenuation control mechanisms and between the *pyrBI* and *pyrF* attenuator-independent control mechanisms suggest that the *pyrBI* operon may have acquired a combination of the control mechanisms of the other two *pyr* genes during the course of evolution. This possibility is of particular interest with respect to the attenuator-independent control mechanisms, of which we know essentially nothing. It suggests that these mechanisms may employ common regulatory elements, a possibility that could facilitate their identification.

## ACKNOWLEDGMENT

This work was supported by Public Health Service grant GM29466 from the National Institutes of Health.

## LITERATURE CITED

- Alper, M. D., and B. N. Ames. 1978. Transport of antibiotics and metabolite analogs by systems under cyclic AMP control: positive selection of *Salmonella typhimurium cya* and *crp* mutants. *J. Bacteriol.* **133**:149–157.
- Bachmann, B. J. 1980. Linkage map of *Escherichia coli* K-12, edition 6. *Microbiol. Rev.* **44**:1–56.
- Bauer, C. E., S. D. Hesse, D. A. Waechter-Brulla, S. P. Lynn, R. I. Gumport, and J. F. Gardner. 1985. A genetic enrichment for mutations constructed by oligodeoxynucleotide-directed mutagenesis. *Gene* **37**:73–81.
- Bonekamp, F., K. Clemmesen, O. Karlström, and K. F. Jensen. 1984. Mechanism of UTP-modulated attenuation at the *pyrE* gene of *Escherichia coli*: an example of operon polarity control through the coupling of translation to transcription. *EMBO J.* **3**:2857–2861.
- Casadaban, M. J. 1976. Transposition and fusion of the *lac* genes to selected promoters in *Escherichia coli* using bacteriophage lambda and mu. *J. Mol. Biol.* **104**:541–555.
- Clemmesen, K., F. Bonekamp, O. Karlström, and K. F. Jensen. 1985. Role of translation in the UTP-modulated attenuation at the *pyrBI* operon of *Escherichia coli*. *Mol. Gen. Genet.* **201**:247–251.
- Feinberg, A. P., and B. Vogelstein. 1983. A technique for radiolabeling DNA restriction endonuclease fragments to high specific activity. *Anal. Biochem.* **132**:6–13.
- Jensen, K. F., R. Fast, O. Karlström, and J. N. Larsen. 1986. Association of RNA polymerase having increased  $K_m$  for ATP and UTP with hyperexpression of the *pyrB* and *pyrE* genes of *Salmonella typhimurium*. *J. Bacteriol.* **166**:857–865.
- Levin, H. L., and H. K. Schachman. 1985. Regulation of aspartate transcarbamoylase synthesis in *Escherichia coli*: analysis of deletion mutations in the promoter region of the *pyrBI* operon. *Proc. Natl. Acad. Sci. USA* **82**:4643–4647.
- Lynn, S. P., L. M. Kasper, and J. F. Gardner. 1988. Contributions of RNA secondary structure and length of the thymidine tract to transcription termination at the *thr* operon attenuator. *J. Biol. Chem.* **263**:472–479.
- Maniatis, T., E. F. Fritsch, and J. Sambrook. 1982. *Molecular cloning: a laboratory manual*. Cold Spring Harbor Laboratory, Cold Spring Harbor, N.Y.
- Maxam, A. M., and W. Gilbert. 1980. Sequencing end-labeled DNA with base-specific chemical cleavages. *Methods Enzymol.* **65**:499–560.
- Messing, J. 1983. New M13 vectors for cloning. *Methods Enzymol.* **101**:20–78.
- Miller, J. H. 1972. *Experiments in molecular genetics*. Cold Spring Harbor Laboratory, Cold Spring Harbor, N.Y.
- Neuhard, J., and P. Nygaard. 1987. Purines and pyrimidines, p. 445–473. *In* F. C. Neidhardt, J. L. Ingraham, K. B. Low, B. Magasanik, M. Schaechter, and H. E. Umberger (ed.), *Escherichia coli* and *Salmonella typhimurium*: cellular and molecular biology. American Society for Microbiology, Washington, D.C.
- Platt, T. 1986. Transcription termination and the regulation of gene expression. *Annu. Rev. Biochem.* **55**:339–372.
- Poulsen, P., and K. F. Jensen. 1987. Effect of UTP and GTP pools on attenuation at the *pyrE* gene of *Escherichia coli*. *Mol. Gen. Genet.* **208**:152–158.
- Roland, K. L., C. Liu, and C. L. Turnbough, Jr. 1988. Role of the ribosome in suppressing transcriptional termination at the *pyrBI* attenuator of *Escherichia coli* K-12. *Proc. Natl. Acad. Sci. USA* **85**:7149–7153.
- Roland, K. L., F. E. Powell, and C. L. Turnbough, Jr. 1985. Role of translation and attenuation in the control of *pyrBI* operon expression in *Escherichia coli* K-12. *J. Bacteriol.* **163**:991–999.
- Sanger, F., S. Nicklen, and A. R. Coulson. 1977. DNA sequencing with chain-terminating inhibitors. *Proc. Natl. Acad. Sci. USA* **74**:5463–5467.
- Schwartz, M., and J. Neuhard. 1975. Control of expression of the *pyr* genes in *Salmonella typhimurium*: effects of variations in uridine and cytidine nucleotide pools. *J. Bacteriol.* **121**:814–822.
- Turnbough, C. L., Jr. 1983. Regulation of *Escherichia coli* aspartate transcarbamylase synthesis by guanosine tetraphosphate and pyrimidine ribonucleoside triphosphates. *J. Bacteriol.* **153**:998–1007.
- Turnbough, C. L., Jr., K. L. Hicks, and J. P. Donahue. 1983. Attenuation control of *pyrBI* operon expression in *Escherichia coli* K-12. *Proc. Natl. Acad. Sci. USA* **80**:368–372.
- Turnbough, C. L., Jr., K. H. Kerr, W. R. Funderburg, J. P. Donahue, and F. E. Powell. 1987. Nucleotide sequence and characterization of the *pyrF* operon of *Escherichia coli* K-12. *J. Biol. Chem.* **262**:10239–10245.
- Winans, S. C., S. J. Elledge, J. H. Krueger, and G. C. Walker. 1985. Site-directed insertion and deletion mutagenesis with cloned fragments in *Escherichia coli*. *J. Bacteriol.* **161**:1219–1221.